Analysis of Probe Surveys Conducted in the 10-MW TP3 Arc-Jet Facility 15-Inch Nozzle Flow

Tahir Gökçen[1]
AMA Inc., NASA Ames Research Center, Moffett Field, CA 94035

Computational simulations and analysis of flow characterization tests in a high enthalpy arc-jet facility at NASA Ames Research Center are reported. These tests were conducted in the 10-MW TP3 facility 15-inch conical nozzle, and pitot pressure and heat flux probes are used to survey test flow downstream of the nozzle exit. Two 1.59-cm (0.625 in) diameter hemisphere probes were used: one with a stagnation-point pressure port, the other with a Gardon heat flux gage. Calibration data were also obtained using 10.16-cm iso-q and 20.32-cm flat-faced slug calorimeters. Experimental surveys of arc-jet test flow with pitot pressure and heat flux probes were obtained at eight arc-heater conditions, covering wide ranges in arc current (316–1756 A) and mass flow rate (32–500 g/s, without any cold-gas injection at the arc-heater plenum) and providing assessment of the flow uniformity in the facility. The present analysis comprises computational fluid dynamics simulations of the nonequilibrium flowfield in the facility nozzle and test box, including the models tested. These simulations take into account non-uniform total enthalpy and mass flux profiles at the nozzle inlet as well as the expansion waves emanating from the nozzle exit and their effects on the model flowfields. Comparisons of computations with the experimental measurements are presented, showing reasonably good agreement. The probe survey data and accompanying analysis show that the test flow in the TP3 15-inch nozzle is highly non-uniform at most conditions, and the extent of flow non-uniformity depends on arc current and mass flow rate.

I. Nomenclature

c_i	=	species mass fraction for species i
D_e	=	nozzle exit diameter, cm (or in)
h	=	enthalpy, MJ/kg
h_o	=	total enthalpy, MJ/kg
h_{ob}	=	mass-averaged total enthalpy (or bulk enthalpy), MJ/kg
h_{ocl}	=	centerline total enthalpy, MJ/kg
I	=	arc current, A
M	=	Mach number
$\dot{m}$	=	total mass flow rate, g/s
$\dot{m}_{N2}$	=	nitrogen flow rate, g/s
$\dot{m}_{O2}$	=	oxygen flow rate, g/s
$\dot{m}_a$	=	cold-gas injection rate at the plenum (N_2), g/s
$\dot{m}_{ar}$	=	argon flow rate, g/s
p	=	pressure, kPa
p_{box}	=	test box pressure, torr
p_{midc}	=	arc-heater mid-column pressure, kPa
p_{anode}	=	arc-heater anode pressure, kPa
$p_{cathode}$	=	arc-heater cathode pressure, kPa
p_o	=	total pressure, kPa
p_{t2}	=	pitot pressure or model stagnation pressure, kPa
q_{GG}	=	1.59-cm hemisphere probe Gardon-gage heat flux, W/cm^2
q_s	=	surface heat flux, W/cm^2

[1] Senior Research Scientist, MS 230-2, Associate Fellow AIAA

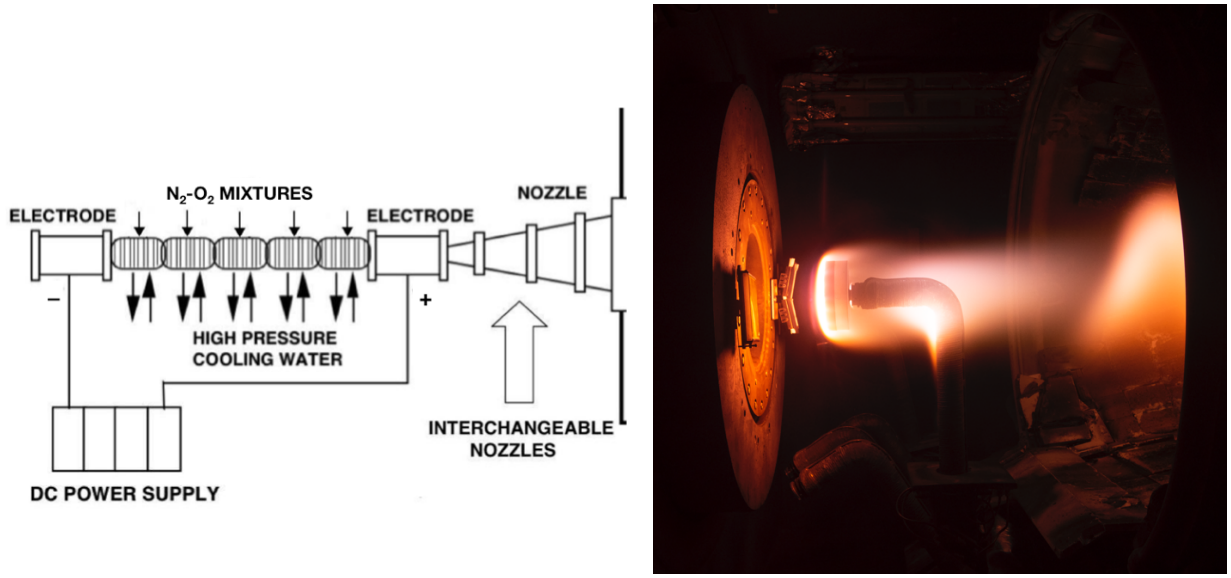
r_c = model corner radius, m
r_n = nose radius, m
s = arc-length coordinate or the survey probe location, m
T = temperature or translational-rotational temperature, K
T_v = vibrational-electronic temperature, K
V = arc voltage, V
x_{ml} = model location from the nozzle exit plane, cm

II. Introduction

Arc-jet facilities provide the primary means to study the performance of various types of thermal protection systems (TPS) used on the outer surfaces of spacecraft in an aerothermodynamic heating environment. In a high enthalpy arc-jet facility, a test gas, usually air or a mixture of nitrogen, oxygen and argon, is passed through an electric arc discharge where the energy is added to the flow. The test gas is then expanded through a converging-diverging nozzle into an evacuated test chamber to produce high-enthalpy supersonic or hypersonic flow. NASA Ames Research Center (ARC) has four arc-jet facilities within its Arc-Jet Complex [1]. One of these arc-jet facilities, the Aerodynamic Heating Facility (AHF), has recently been upgraded to run with a 10-MW constricted arc heater, named the TP3, which was formerly known as the TP2 when operated at Johnson Space Center [2]. The TP3 currently operates with a test gas mixture of pure nitrogen and variable oxygen without argon gas (with mixtures of nitrogen and carbon dioxide planned in the future) [3].

Among the various arc-jet test configurations available at Ames, the TP3 uses a conical nozzle test configuration, in which stagnation pucks or wedge models are placed in a free jet downstream of the nozzle exit. Although the TP3 has been operational at Ames since 2013 [3], and flow characterization studies were already performed in the TP3 7.5-inch nozzle [4, 5], the TP3 15-inch nozzle was used the first time in the AHF in 2019. For flow characterization purposes, pitot pressure and heat flux probes are used to survey the test flow downstream of the 15-inch nozzle exit at a wide range of arc-heater conditions, providing assessment of the flow uniformity in the facility with this nozzle.

The present analysis comprises computational fluid dynamics (CFD) simulations of the nonequilibrium flowfield in the facility nozzle and test box, including the models tested. CFD simulations take into account non-uniform total enthalpy and mass flux profiles at the nozzle inlet as well as the expansion waves emanating from the nozzle exit and their effects on the model flowfields. Comparisons of CFD simulations with the experimental measurements are presented. Based on the probe survey data and CFD analysis, assessment of the flow uniformity in the TP3 15-inch nozzle is assessed.



(a) arc-heater/nozzles sketch **(b) flat-faced model test**

Figure 1. TP3 sketch and a photograph of TP3 15-inch nozzle test.

III. Arc-Jet Facility and Tests

The AHF at ARC, with its 10-MW TP3 constricted arc-heater configuration, is designed to operate with a set of conical nozzles. All of the nozzles have the same inlet diameter of 10.16 cm (4 in), and the same throat diameter of 5.715 cm (2.25 in). Nozzle exit diameters range from 12.7 cm to 101.6 cm (5, 7.5, 10, 15, 20, and 40 in). The diverging section of each nozzle has a half-angle of 15° [1, 3]. Figure 1 shows a schematic diagram of a wall-constricted arc-jet with its interchangeable nozzles and a photograph of a flat-faced model test in the TP3 15-inch nozzle.

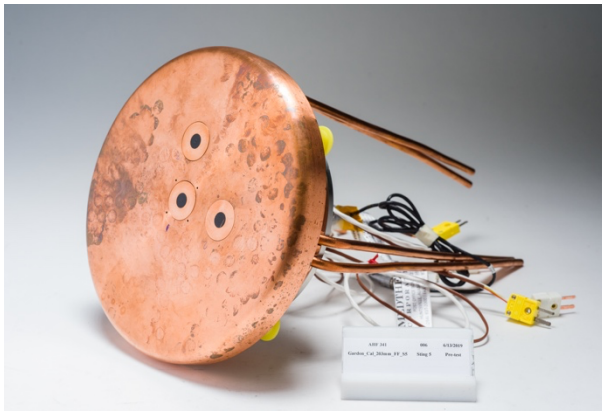
The present probe survey data were obtained in the TP3 15-inch diameter conical nozzle during the AHF 341 test series in 2019. The pitot pressure and Gardon-gage heat flux surveys of the nozzle jet in the test section were done at eight arc-jet conditions and at about 20.3 cm distance from the nozzle exit. Each condition was calibrated separately for its centerline conditions with 20.3-cm diameter flat-faced slug calorimeters (the same shape as the test article). The shoulder region of the flat-faced models is rounded to the cylindrical sides (r_c=0.95 cm). These surveys were performed using 1.59-cm diameter hemisphere probes (D=0.625 in). Two survey probes were used: one with a stagnation-point pressure port, the other with a Gardon heat flux gage. The sweeps to survey across the nozzle were done by moving the probes horizontally across the free jet in two directions: first from east to west, then retracting back west to east. This provides two experimental data sets for each survey sweep. Figure 2 shows photographs of the pitot pressure and heat flux survey probes and calorimeter models. Additional information on the heat flux measurement techniques and standards can be found in [6-8].



(a) 1.59-cm hemisphere pitot probe and Gardon gage calorimeter



(b) 20.3-cm flat-faced slug calorimeter



(c) 20.3-cm flat-faced Gardon gage calorimeter

Figure 2. Photographs of the survey probes and calorimeter models used to calibrate arc-jet test conditions.

One important testing capability of the 10-MW TP3 facility is its ability to simulate various heating profiles in time representative of hypersonic flight. In a heating profile test, the heating profile is usually broken into a number of independent steps where each step is calibrated using calorimeters for its centerline conditions prior to the profile run, and subsequently the heating profile simulation is carried out in a single arc-jet run. Since the facility configuration is fixed, achieving the wide range of conditions needed in the heating profile simulation requires that the facility operate at the extremes of its operating envelope. The flight profile simulation and its results are outside the scope of this

paper. The reason it is mentioned here is that the arc-jet conditions presented were actual steps in various flight heating profile simulations in AHF 341 tests. There was no other rationale in choosing these conditions for the probe surveys. However, it should be noted that these conditions cover wide ranges in arc current (316–1756 A) and mass flow rate (32–500 g/s), and do not include any cold-gas injection at the arc-heater plenum, providing assessment of the flow uniformity in the facility. Nominal facility parameters for the eight conditions are given in Table 1. Note that these cases are ordered such that they are increasing with increasing mass flow rate and arc current.

Table 1. Summary of nominal facility conditions for the probe sweeps in the TP3 15-inch nozzle (AHF 341).

AHF 341 condition	Case 1 10n	Case 2 3	Case 3 4	Case 4 5	Case 5 11n	Case 6 9n	Case 7 7n	Case 8 2
p_{midc}, kPa	40	39	72	264	287	402	433	522
I, A	316	401	804	1204	598	696	902	1756
V, V	1386	1327	1828	3626	4526	5257	5140	4861
$\dot{m}$, g/s	33	32	60	250	350	500	500	500
$\dot{m}_{N2}$	23	23	46	193	270	385	385	385
$\dot{m}_{O2}$	7	7	14	57	80	115	115	115
$\dot{m}_{N2plenum}$	0	0	0	0	0	0	0	0
$\dot{m}_{Ar}$	3	2	0	0	0	0	0	0

IV. Computational Approach

Computational analyses of arc-jet tests are performed through simulation of nonequilibrium expanding flow in the arc-jet nozzle and supersonic jet, and simulation of the flow in the test box and around the test articles. For all CFD calculations, the Data Parallel Line Relaxation (DPLR) code [9, 10], a NASA Ames in-house flow solver, is used. DPLR has been employed extensively at Ames for hypersonic flight, planetary entry and arc-jet simulations. DPLR provides various options for thermophysical models and formulation. For CFD calculations presented in this paper, two-dimensional axisymmetric or three-dimensional Navier-Stokes equations, supplemented with the equations accounting for nonequilibrium kinetic processes, are used in the formulation. The thermochemical model employed for the arc-jet flow includes five species (N_2 O_2, NO, N, O), or six species (N_2 O_2, NO, N, O, Ar) when argon is present, and the thermal state of the gas is described by two temperatures (translational-rotational and vibrational-electronic) within the framework of Park's two-temperature model [11].

The flowfield in an arc-jet facility, from the arc heater to the test section, is a very complex, three-dimensional flow with various nonequilibrium processes occurring. In order to simulate the flowfield, several simplifying assumptions are made, and corresponding numerical boundary conditions are prescribed for CFD simulations. The present computational approach follows our earlier work [5, 12, 13], and it is also briefly described here. Simulations of the arc-jet facility flow are started from the nozzle inlet. The total enthalpy and its radial profile at the inlet are prescribed based on the facility and calibration data, and the flow properties at the inlet are assumed to be in thermochemical equilibrium. Measured facility data, namely the total pressure, mass flow rate, and test box pressure, are used as boundary conditions.

V. Computational Results

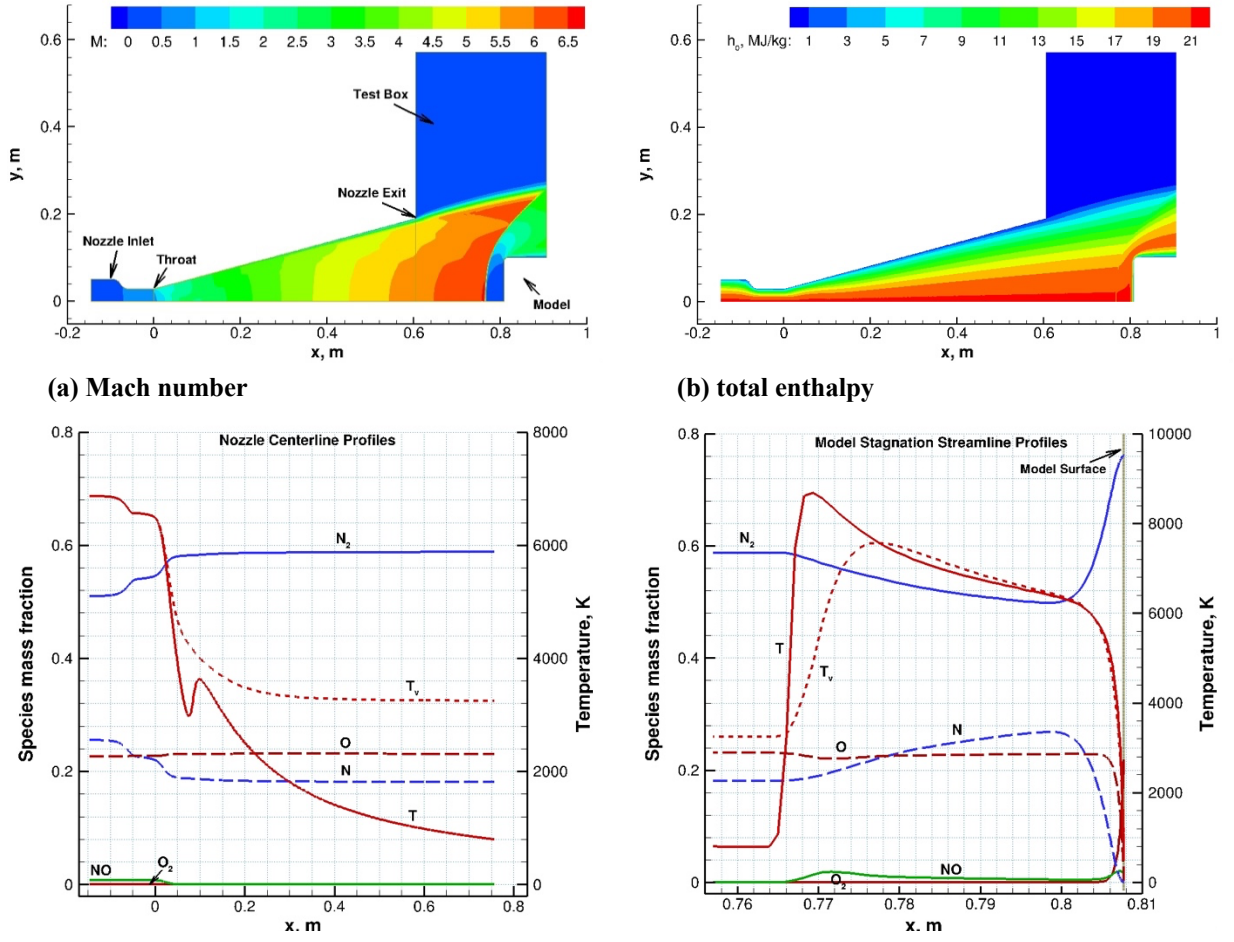
First, one flat-faced stagnation model simulation is presented. Then, comparisons of computations with the pitot pressure and Gardon-gage heat flux surveys obtained in the TP3 15-inch nozzle are presented.

A. Stagnation calorimeter simulations

Stagnation calorimeters, typically with the same geometry of test articles, are used to calibrate the arc-jet test conditions. As in our previous work, these calorimeter measurements along with the facility data and CFD simulations

are then used to infer the centerline total enthalpy of the arc-jet flow. In order to estimate the centerline total enthalpy with CFD simulations, uniform pressure and a non-uniform parabolic enthalpy profile are specified at the nozzle inlet such that the calorimeter measurements are reproduced with the computations. This approach also used in our earlier work [5, 12, 14] is analogous to the ASTM standard E637-05 [15], except that the calorimeter surface heat flux and pressure are predicted by CFD simulations, replacing the heat transfer theory used in the standard.

As an illustration of a typical calorimeter simulation, Fig. 3 shows a computed TP3 15-inch nozzle flowfield including the test box and a flat-faced calorimeter model. In Fig. 3a and 3b, computed Mach number and total enthalpy contours are shown. In order to provide some insight into the nonequilibrium flowfield chemistry within the nozzle and shock layer formed in front of the calorimeter model, species mass fraction and temperature profiles are shown (Fig. 3c and 3d). Because of the nonequilibrium expansion process in the nozzle, the chemical composition freezes near the throat where the flow is dissociated and vibrationally excited. For this case, at this pressure and moderately high enthalpy level, the computations predict that the flow is chemically frozen but remains in vibrational nonequilibrium before it reaches the nozzle exit (Fig. 3c). Note that oxygen remains fully dissociated within the entire flowfield except in the boundary layer near the walls, while nitrogen is partially dissociated. In Fig. 3d, further dissociation of N_2, vibrational relaxation, followed by thermal equilibration are predicted along the model stagnation streamline.



(a) Mach number **(b) total enthalpy**

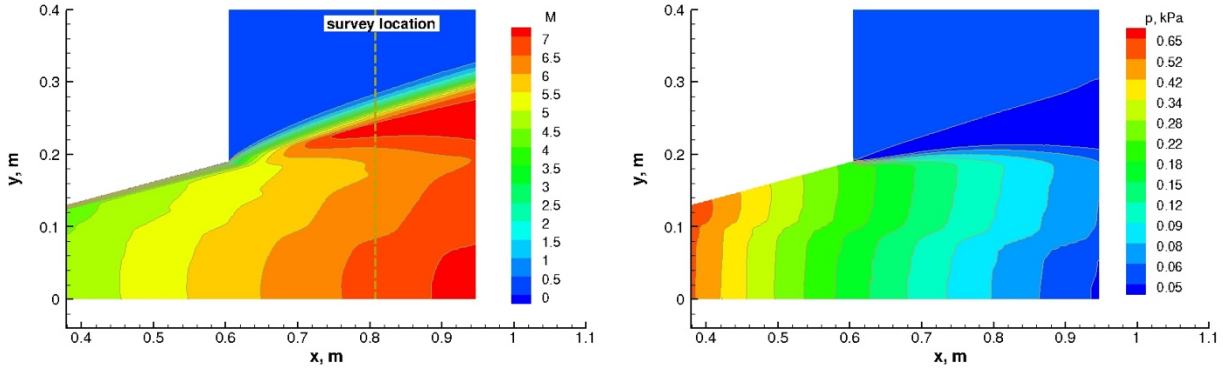
(c) nozzle centerline **(d) stagnation streamline**

Figure 3. Computed TP3 15-inch nozzle flowfield including the test box and a 20.3-cm diameter flat-faced calorimeter model: $\dot{m}$ = 250 g/s, h_{ob} = 11.4 MJ/kg, h_{ocl} = 21.3 MJ/kg, parabolic enthalpy profile, N_2/O_2 mixture, p_{box} = 1 torr.

B. Comparisons with pitot pressure and heat flux survey data

Comparisons of CFD simulations with the survey data follow the approach presented in [4, 5, 11]. While the data obtained from the pitot pressure surveys are used as quantitative data, Gardon gage heat flux measurements from the probe surveys are used as qualitative data since they were not consistent with the slug calorimeter data. Therefore, only normalized distributions of the heat flux measured by the survey probes are used in comparisons with computations. Furthermore, since direct comparisons would require three-dimensional CFD simulations of flowfields around the survey probes at several locations in the test section, only approximate comparisons are made based on the computed axisymmetric CFD flowfields. Quantitative pitot pressure comparisons are based on the CFD flowfield and shock relations (pressure, Mach number, frozen flow). For normalized heating distribution comparisons, the heat flux from the Gardon gage probes is assumed to be proportional to $h_o p_{t2}^{1/2}$, and corresponding computations are based on the CFD flowfield.

For an example, Fig. 4 shows the computed Mach number and pressure contours near the nozzle exit and supersonic jet for the case shown in Fig. 3. These simulations do not include the model in the test box. It should be noted that the expansion of the jet exiting the nozzle and the width of the jet are controlled by the test box pressure [10]. On the Mach number contour plot, the probe survey location is also indicated. The axial location for the survey probes is approximately at x = 0.806 m or at x_{ml} = 20.32 cm (8 inches downstream of the nozzle exit).



(a) Mach number **(b) pressure**

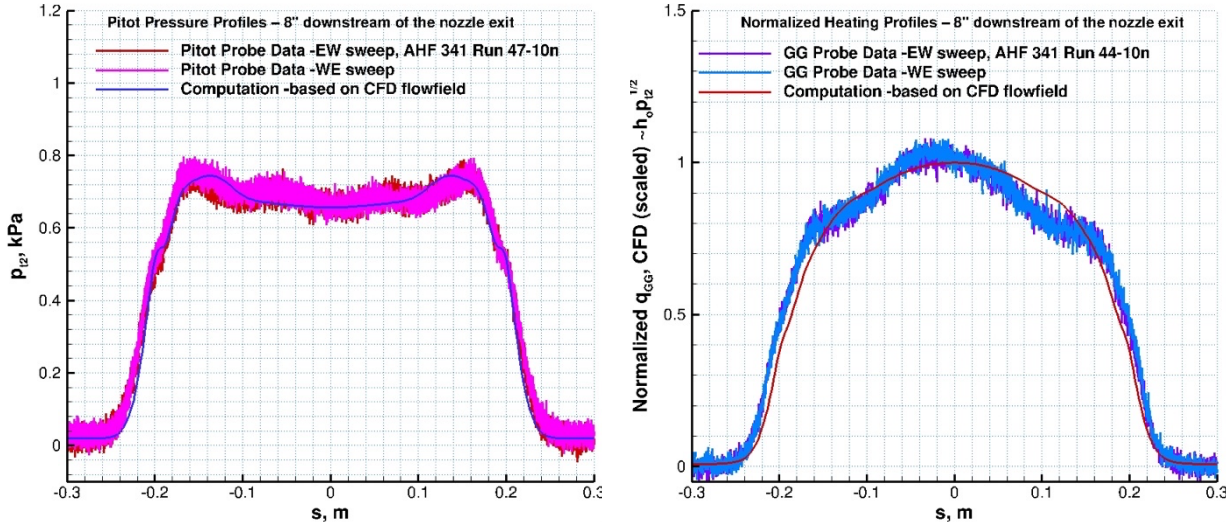
Figure 4. Computed flowfield contours near the nozzle exit and test box, and axial location for the survey probes. TP3 15-inch nozzle flow: $\dot{m}$ = 250 g/s, h_{ob} = 11.4 MJ/kg, h_{ocl} = 21.3 MJ/kg, parabolic enthalpy profile, N_2/O_2 mixture, p_{box} = 0.4 torr.

Comparisons of computations with the pitot pressure and Gardon-gage heat flux survey data will be presented for three cases (1, 4 and 8) listed in Table 1. These three cases correspond to the minimum, an intermediate and the maximum facility conditions in terms of arc current and mass flow rate. The proposed paper will include comparisons for all conditions. Note that for each condition, the centerline total enthalpy value is set such that centerline stagnation calorimeter data, surface pressure and heat flux are reproduced with CFD calculations. Also, the pitot pressure and heat flux survey data were obtained in separate arc-jet runs but at the same nominal facility conditions listed in Table 1.

Case 1, AHF 341 condition 10n (316 A, 33 g/s): minimum arc current and mass flow rate

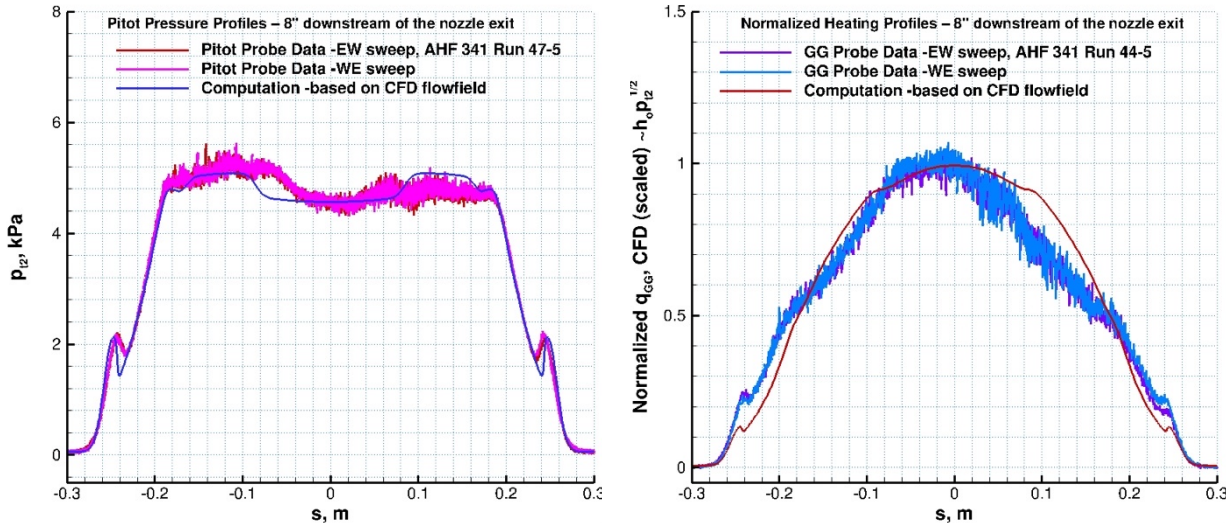
This condition represents a facility condition at the minimum arc current and mass flow rate, and there is no plenum cold gas injection. Figure 5 shows comparisons of computations with the pitot pressure and Gardon-gage heat flux survey data. Note that the sweep data obtained, both pitot pressure and heat flux data, are repeatable within the measurement fluctuations in both sweep directions (East to West and West to East). In Fig. 5, CFD simulations reproduce the pitot pressure and heat flux data reasonably well. Note also that there appears to be some variation in

the pitot pressure near the nozzle centerline, possibly resulting from weak wave interactions in the supersonic jet. For this case, the enthalpy distribution in the test flow can be considered moderately non-uniform (the centerline-to-bulk enthalpy ratio is 1.43).



(a) pitot pressure **(b) normalized heat flux**

Figure 5. Comparisons of computations with the pitot pressure and heat flux survey data at x_{ml} = 20.3 cm location (Case 1). TP3 15-inch nozzle flow: $\dot{m}$ = 33 g/s, h_{ob} = 9.5 MJ/kg, h_{ocl} = 13.6 MJ/kg, parabolic enthalpy profile, N_2/O_2 mixture with 6.3% Ar, p_{box} = 0.15 torr.



(a) pitot pressure **(b) normalized heat flux**

Figure 6. Comparisons of computations with the pitot pressure and heat flux survey data at x_{ml} = 20.3 cm location (Case 4). TP3 15-inch nozzle flow: $\dot{m}$ = 250 g/s, h_{ob} = 11.4 MJ/kg, h_{ocl} = 21.3 MJ/kg, parabolic enthalpy profile, N_2/O_2 mixture, p_{box} = 0.4 torr.

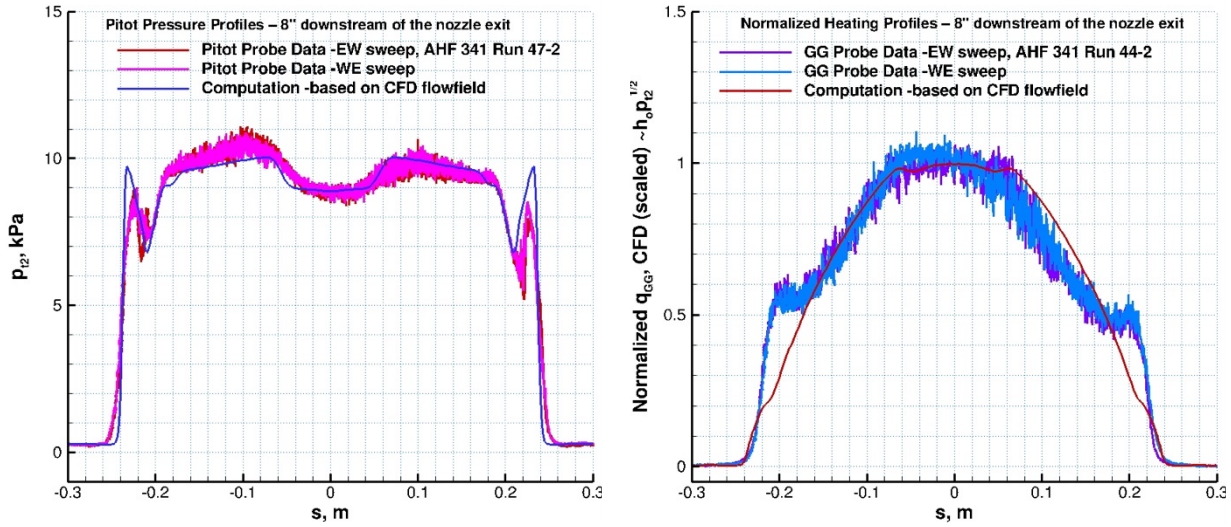
Case 4, AHF 341 condition 5 (1204 A, 250 g/s): moderately high arc current and intermediate mass flow rate

This facility condition is at moderately high arc current and intermediate mass flow rate, with no plenum cold gas injection. Figure 6 shows comparisons of computations with the pitot pressure and Gardon-gage heat flux survey

data. Again, both pitot pressure and heat flux sweep data are repeatable in both sweep directions (EW and WE). However, both pitot and heat flux survey data are slightly asymmetric with respect to the nozzle/jet centerline. More importantly, the measured pitot pressure profile, as well as the CFD computations, both show a dip near the jet centerline. This non-uniform flow feature observed in the pitot surveys is primarily due to the TP3 nozzle throat design. For the elongated throat design, expansion waves are generated at the throat and diverging-nozzle cone intersection, and these waves propagate downstream and reflect on the nozzle centerline as compression waves (eventual shock formation). These waves are observed in the computed Mach number contours in Fig. 3a and Fig. 4a, as well as in the pressure contours in Fig. 4b. (The proposed paper will have additional simulation results to clarify this wave formation and its possible mitigation.) It is also worth mentioning here that the features in the pitot and heat flux surveys at s ~ ±0.25 m correspond to the nozzle jet boundary (see Fig. 4a), the location of which is primarily determined by the test box pressure. Again, CFD simulations reproduce the pitot pressure and heat flux data reasonably well. For this case, the enthalpy distribution in the test flow is considered highly non-uniform (the centerline-to-bulk enthalpy ratio is 1.87).

Case 8, AHF 341 condition 2 (1756 A, 500 g/s): maximum arc current and high mass flow rate

This facility condition is at the maximum arc current and relatively high mass flow rate, with no plenum cold gas injection. Although somewhat higher mass flow rates are possible for the TP3 heater, for AHF 341 tests, this condition was considered as the maximum facility condition (maximum current and maximum flow rate). For this case, Fig. 7 shows comparisons of computations with the pitot pressure and Gardon-gage heat flux survey data. Again, both pitot pressure and heat flux sweep data are repeatable between EW and WE sweep directions, and both are slightly asymmetric with respect to the jet centerline. The non-uniform flow feature or the dip in the pitot survey data near the jet centerline that was discussed in Case 4 is also clearly observed for this case. Although CFD simulations reproduce the pitot pressure data well including the dip, they underpredict the heat flux distribution near the jet boundary. As mentioned earlier, the heating distribution near the jet boundary is significantly affected by the test box pressure. Sensitivity of the pitot pressure and heat flux surveys to the test box pressure will be included in the proposed paper. Again, since the centerline-to-bulk enthalpy ratio is about 2.23, the enthalpy distribution in the test flow for this case is considered highly non-uniform.



(a) pitot pressure **(b) normalized heat flux**

Figure 7. Comparisons of computations with the pitot pressure and heat flux survey data at x_{ml} = 20.3 cm location (Case 8). TP3 15-inch nozzle flow: $\dot{m}$ = 500 g/s, h_{ob} = 12.9 MJ/kg, h_{ocl} = 28.8 MJ/kg, parabolic enthalpy profile, N_2/O_2 mixture, p_{box} = 2 torr.

From these three cases, the probe survey data along with CFD analysis show that the test flow in the TP3 15-inch nozzle is highly non-uniform at most conditions. As expected, the extent of flow non-uniformity, or the inferred centerline-to-bulk enthalpy ratio, depends on facility conditions (arc current and mass flow rate). As mentioned earlier, proposed paper will include analysis and comparisons with the test data for eight conditions.

Acknowledgments

This work was funded by the NASA Orion TPS Insight/Oversight project. The arc-jet operational capability at NASA ARC is also supported by NASA-SCAP. The author would like to thank AHF 341 test PIs, Eric Espesito (Lockheed Martin), Antonella Alunni, and Shahab Salehghaffari, and the TSF test engineers, Enrique Carballo and Imelda Terrazas-Salinas. The support from the NASA Ames Entry Systems and Technology Division, through contract NNA15BB15C to AMA, Inc., is gratefully acknowledged.

References

[1] Terrazas-Salinas, I., and the staff of Thermophysics Facilities Branch, "Test Planning Guide for NASA Ames Research Center Arc-Jet Complex and Range Complex," A029-9701-XM3 Rev. D, Entry Systems and Technology Division, NASA Ames Research Center, January 2018.

[2] Rochelle, W. C., Battley, H. H., Grimaud, J. E., Tillian, D. J., Murray, L. P., Lueke, W. J., and Heaton, T. M., "Orbiter TPS Development and Certification Testing at the NASA/JSC 10 MW Atmospheric Reentry Materials and Structures Evaluation Facility," AIAA-83-0147, Jan. 1983.

[3] Balboni, J. A., Gökçen, T., Hui, F. C. L., Graube, P., Morrissey, P., Lewis, R. "Consolidating NASA's Arc-Jets," AIAA Paper 2015-2667, June 2015.

[4] Gökçen, T., Balboni, J. A., and Alunni, A. I. "Computational Simulations of the 10-MW TP3 Arc-Jet Facility," AIAA Paper 2015-3103, June 2015.

[5] Gökçen, T., and Alunni, A. I., "Flow Characterization Studies of the 10-MW TP3 Arc-Jet Facility: Probe Sweeps," AIAA Paper 2016-4153, June 2016.

[6] Terrazas-Salinas, I., Carballo, J. E., Driver, D. M., and Balboni, J. A., "Comparison of Heat Transfer Measuremen Devices in Arc Jet Flows with Shear," AIAA Paper 2010-5053, June 2010.

[7] ASTM E457-96, "Standard Test Method for Measuring Heat-Transfer Rate Using a Thermal Capacitance (Slug) Calorimeter," American Society for Testing and Materials, Ocober 1996 (Reapproved 2002, originally published in 1972).

[8] ASTM E511-07, "Standard Test Method For Measuring Heat Flux Using a Copper-Constantan Circular Foil Heat-Flux Gage," American Society for Testing and Materials, December 2007 (original standard published in 1973).

[9] Wright, M. J., Candler, G. V., and Bose, D., "Data-Parallel Line Relaxation Method for the Navier-Stokes Equations," *AIAA Journal*, Vol. 36, No. 9, 1998, pp. 1603-1609.

[10] Wright, M. J., "Data-Parallel Line Relaxation Code, DPLR Version 4.02," Private Communication, June 2010.

[11] Park, C., *Nonequilibrium Hypersonic Aerothermodynamics*, John Wiley & Sons, Inc., New York, 1990, Chap. 4.

[12] Gökçen, T., Chen, Y. K., Skokova, K. A., and Milos, F. S., "Computational Analysis of Arc-Jet Stagnation Tests Including Ablation and Shape Change," *Journal of Thermophysics and Heat Transfer*, Vol. 24, No. 4, 2010, pp. 694-707; also AIAA Paper 2009-3596, June 2009.

[13] Gökçen, T., "Effects of Test Box Pressure on Arc-Jet Flowfields and Implications for Testing," AIAA Paper 2018-3771, June 2018.

[14] Gökçen, T., and Alunni, A. I., "CFD Simulations of the IHF Arc-Jet Flow: 9-Inch Nozzle, Flow Surveys, LEAF Wedge Calibration Data," AIAA Paper 2019-3008, June 2019.

[15] ASTM E637-05, "Standard Test Method for Calculation of Stagnation Enthalpy from Heat Transfer Theory and Experimental Measurements of Stagnation-Point Heat Transfer and Pressure," American Society for Testing and Materials, November 2005 (originally published in 1978).